

# Empirical Validation of a Model for Predicting the Compressive Strength of Cemented Rockfill: Advancing Quality Control Methodologies

Ghada Rafrat<sup>1,3</sup>, Tikou Belem<sup>1</sup>, Louis-Philippe Gélinas<sup>2</sup>, Hatem Mrad<sup>1</sup>, Abdelkader Krichen<sup>3</sup>

<sup>1</sup>Université du Québec en Abitibi-Témiscamingue (UQAT), Rouyn-Noranda, PQ, Canada, [ghada.rafrat@uqat.ca](mailto:ghada.rafrat@uqat.ca); [tikou.belem@uqat.ca](mailto:tikou.belem@uqat.ca); [hatem.mrad@uqat.ca](mailto:hatem.mrad@uqat.ca)

<sup>2</sup>Agnico Eagle Mines Limited, Support and Development Center (CSD), Rouyn-Noranda, PQ, Canada, [Louis-Philippe.Gelinas@agnicoeagle.com](mailto:Louis-Philippe.Gelinas@agnicoeagle.com)

<sup>3</sup>Université de Sfax, École Nationale d'Ingénieurs de Sfax (ENIS), Sfax, Tunisia, [krichenabdelkader@yahoo.fr](mailto:krichenabdelkader@yahoo.fr)

## Abstract:

To tackle the issues associated with mine waste management, adopting a sustainable strategy involves repurposing solid waste into raw materials. This practice contributes to the development of conventional mine backfills, notably cemented rockfills (CRFs). CRFs are widely employed in the mining sector due to their capacity to deliver high unconfined compressive strength (UCS) and ensure effective ground stability and control. Despite their prevalence, the intricate preparation procedures, and diverse composition of CRFs have hindered their broad acceptance. Moreover, the lack of a systematic design to facilitate binder usage control for CRFs further exacerbates this challenge in the mining industry.

The objective of this study is to develop a thorough technical quality control procedure for CRF mixtures, with a specific focus on predicting their compressive strength. The methodology encompasses the initial empirical validation and calibration of an existing semi-empirical model, utilizing laboratory-prepared mixtures with diverse formulations. Once successfully validated, the semi-empirical model is intended for broader application through the creation of a user-friendly application for predicting constants. Subsequently, a pragmatic quality control (QC) procedure of CRF will be implemented, integrating fundamental relations and gravimetric water content determination.

The outcomes illustrate the reliability of the semi-empirical model in predicting the UCS of CRF and cement slurry. This predictive capacity underwent assessment through linear regressions, revealing coefficients close to 1. An application has been devised to forecast parameters associated with the type of cement used in CRF mixtures, streamlining the prediction of suitable values based on experiment-related data. Furthermore, the results emphasize the importance of vigilant monitoring of geotechnical parameters (final wet density, dry density, gravimetric water content) and a meticulous selection of components for cemented rockfill mixtures to uphold their stability.

Key words: cemented rockfill, unconfined compressive strength, semi-empirical predictive model, empirical validation, CRF mixtures formulation, quality control

## Introduction

Recent research indicates that ongoing mining operations and geological exploration in the Province of Quebec have a direct impact on the growth of its Gross Domestic Product (GDP). According to expert estimates using 2018 data, the mining sector's overall contribution to the GDP was approximately 9 billion C\$ (Quebec Mining Association - QMA, 2019). Despite being a major contributor to GDP development, the mining industry generates a substantial amount of solid waste that can be reactive, leading to acidic

water formation (Bussière, 2007; Aubertin et al., 2002; Amaratunga and Yaschyshyn, 1997). In response to this environmental challenge, the mining sector has adapted its underground mining methods by recycling waste as structural components. This adjustment aims to minimize the environmental hazards associated with surface storage of solid waste, particularly of secondary ground support.

Fine tailings can find application as either paste fill or hydraulic fill, while waste rock can be utilized as rock fill depending on the mining method employed. To achieve this, the mining industry requires appropriate, reliable, and validated analytical tools to evaluate the stability and strength of backfill accurately, especially rockfills. Presently, due to technological advancements, mining operation are reaching unprecedented depths (eg, > 2.5 km at the LaRonde mine in Abitibi-Témiscamingue region), resulting in highly elevated natural stresses induced by ore extraction. These conditions can lead to localized seismic events causing vibrations in the rock, which can have detrimental consequences for the mine. Despite the satisfactory performance of CRF, this type of backfill is often inadequately designed and not fully exploited (Gonano et al., 1978; Yu, 1989; Stone, 1993; Hedley, 1995; Farsangi et al., 1996; Farsangi, 1996; Annor, 1999; Hane et al., 2018). Through the literature, several authors have proposed empirical and semi-empirical models for predicting the UCS of CRFs, primarily based on the binder ratio by mass, the water-to-cement ratio, and the expected porosity of the mixture (Mitchell & Wong, 1982; Arioglu, 1984; Yu, 1989; Lamos & Clark, 1993; Hedley, 1995; Annor, 1999; Belem, 2020).

### Existing semi-empirical models

In order to develop a tool to assist in the formulation of CRFs, a semi-empirical model for predicting the UCS of CRFs was developed at the Research Institute of Mines and Environment (RIME). This model is presented as follows (Belem, 2020, *pers. comm.*; Rafrat et al., 2023):

$$UCS_{pred} = A_c \times G_{s-WR} \left( \frac{D_{50}}{D_{min}} \right)^{-n} \left[ \left[ 1 + t_r \right]^{-1.625} \left[ 1 + \left( \frac{W}{C} \right)^{-2} + (B_{w\%})^{1.5} \right]^{-2} \right]^{-m} \quad \text{Equation 1}$$

where,  $A_c$  represents the “critical” unconfined compressive strength of the intact rock forming the waste rock (kPa);  $G_{s-WR}$  denotes the specific gravity of the waste rock;  $D_{50}/D_{min}$  is the particle size ratio between the median and the minimal particle size ( $D_{min}$  is fixed at 10 mm for fine particles);  $t_r$  signifies the relative curing time, calculated as ( $t/10$  days), where  $t$  is the curing time in days;  $W/C$  represents the water-to-cement ratio,  $B_{w\%} = 100 \times mass_{binder}/mass_{waste-rock}$  is the binder rate;  $n$  and  $m$  are the particle size adjustment factor and exponent, respectively, expressing the effect of the binder type. These values are determined empirically.

The performance of this semi-empirical model was tested using preliminary experimental data. While the model accounts for geomechanical characteristics and exhibits promise in predicting uniaxial compressive strength, limitations arise concerning its sensitivity to changes in these parameters. More specifically, the model appears to be weakly sensitive to changes in the  $W/C$  ratio, particularly within the industry-recommended range of 0.7–1.2, or the diameters  $D_{50}$  and  $D_{min}$  (Rafrat et al., 2023). Additionally, minimal variations in UCS values are noted when adjusting the median particle size ( $D_{50}$ ) during model testing for the formulation of cemented rock fill mixtures. This observation indicates a limited impact on uniaxial

compressive strength. In summary, although the model displays some capabilities, it falls short in predicting the strength of neat cement strength after hardening.

To address the shortcomings of the original model for predicting the UCS of CRFs (Belem, 2020, *personal communication*; Rafrat et al., 2023), a significantly enhanced version of the model has been proposed. This improved model, which can predict the compressive strength of both hardened neat cement and cemented rockfill, is given as follows (Belem, 2023, *pers. comm.*):

$$UCS_{pred}(j) = (\gamma_{bulk,j})^\lambda h_r \left[ b f_{GSD} (r_d)^m + \left( 1 + b \left[ f_{GSD} B_{w\%} (r_d)^{-m} \right] \right) \alpha_{ij} \left( \frac{W}{C} \right)^{-d} \sqrt{t_R} \right] \quad \text{Equation 2}$$

and

$$f_{GSD} = 1 + \exp \left( -\frac{1}{4} \left[ \frac{\%P_{10mm} - \mu}{\sigma} \right]^2 \right) \quad \text{Equation 3}$$

where,  $\gamma_{bulk,j}$  (kN/m<sup>3</sup> or kPa/m) is the bulk or total unit weight of waste rock or neat cement slurry;  $\lambda$  is unit weight adjustment factor for model calibration with experimental;  $h_r$  (m) is representative elementary height (REH);  $b$  is the parameter for selecting neat cement ( $b = 0$ ) or CRF ( $b = 1$ ) in the model;  $f_{GSD}$  is the weighting factor for the contribution of fine particles (their proportion) to the strength development (a Gaussian-type function with mean value  $\mu$  and standard deviation  $\sigma$ , see Equation 2), where  $\%P_{10mm}$  is the percentage of particles with a diameter smaller than 10 mm (fines);  $r_d = D_{max}/D_{min}$  is the particle size ratio between the maximal ( $D_{max}$ ) and the minimal ( $D_{min}$ ) particle size ( $D_{min}$  is fixed at 10 mm for fine particles);  $B_{w\%}$  is the binder ratio;  $\alpha_{ij}$  = weighting factor for the mixture:  $i$  = binder type (Portland cements GU or HE, GU-FA, GU-Slag, etc.) and  $j = 1$  for CRF or  $j = 0$  for neat cement slurry (if  $j = 0$  then  $b = 0$ , and if  $j = 1$  then  $b = 1$ );  $W/C$  is the water-to-cement ratio;  $t_R$  is the relative curing time ( $= t/t_0$ , where  $t$  = target curing time and  $t_0$  = reference curing time and  $t_0 = 1$  day).

Figure 1 depicts the Gaussian evolution curve of the parameter  $f_{GSD}$  as a function of the percentage of fine particles ( $D < 10$  mm) with a mean value centered at the optimal proportion,  $\mu = 30\%$ , and a standard deviation of the fine particles proportion,  $\sigma = 5\%$ , based on the ideal particle size distribution curve model. Ideal particle size distribution curves can be used as the target for modifying the size distribution of combinations of classes. The ideal curves are assumed to lead to the optimal packing of granular mixtures (Fuller and Thompson, 1907; Talbot and Richard, 1923), where  $D$  is the opening size of a sieve,  $D_{max}$  is the maximum particle size and  $P(D)$  is the fraction of the material that passes a sieve with the opening size of  $D$ . The value of  $q$  was initially considered constant and equal to 0.5 by Fuller and Thompson (1907). This optimal proportion ( $\mu = 30\%$ ) was set according to the shape of the Fuller-Thompson or Talbot-Richard curve with  $q = 0.5$ . Table 1 presents different values of model parameters.

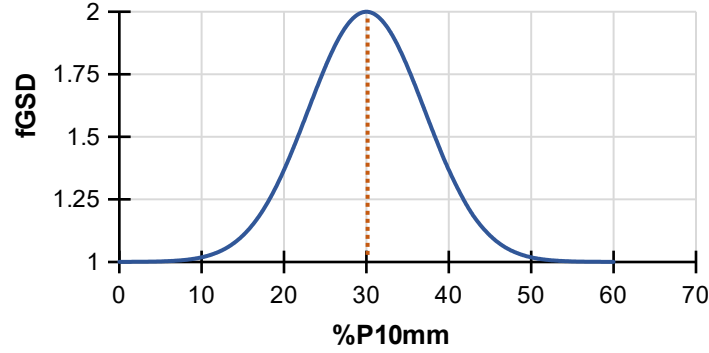


Figure 1. Parameter  $f_{GSD}$  Gaussian curve as a function of the percentage of fine particles.

Table 1. Empirical values of the model's parameters applicable to both CRF and neat cement slurry.

Parameter		Neat cement slurry ( $j = 0$ ; $b = 0$ )	CRF ( $j = 1$ ; $b = 1$ )
Void ratio	$e_{WR}$	–	0.3
Porosity	$n_{WR}$	–	0.232
Water content	$w_{WR}$	–	$\sim 0.02$
constant	$m$	–	0.35
REH	$h_r(m)$	4	4
Factor	$\lambda$	0.978	2.12
constant	$b$	0	1
Factor	$\alpha_i$	Undefined	Undefined
Constant	$d$	1.5	1.5

Equation 2 allows for predicting the UCS of the CRF for a given curing time ( $t$ ), given the binder ratio ( $B_w$  %), as well as the water-to-cement ratio ( $W/C$ ) to be used (along with the CRF placement porosity,  $n_{WR}$ ). Moreover, this semi-empirical model could also be rearranged so that it could be used for the formulation of optimal CRF recipes. To achieve this, it should allow predicting the optimal binder ratio ( $B_{w\%-optimal}$ ) knowing the target water-to-cement ratio ( $W/C$ )<sub>target</sub> and ( $UCS$ )<sub>target</sub> (see Equation 4), or predicting the optimal water-to-cement ratio ( $W/C$ )<sub>optimal</sub> knowing the target binder ratio ( $B_{w\%-target}$ ) and ( $UCS$ )<sub>target</sub> (see Equation 5):

$$(B_{w\%})_{optimal} = \frac{(r_d)^m}{f_{GSD}} \left[ \frac{\left(\frac{W}{C}\right)_{target}^d}{\alpha_i \sqrt{t_R}} \left( \frac{UCS_{target}}{(\gamma_{bulk})^2 h_r} - f_{GSD} (r_d)^m \right) - 1 \right]$$

Equation 4

$$\left(\frac{W}{C}\right)_{\text{optimal}} = \left[ \frac{\frac{UCS_{\text{target}}}{(\gamma_{\text{bulk}})^2 h_t} - f_{\text{GSD}} (r_d)^m}{1 + \frac{f_{\text{GSD}}}{(r_d)^m} B_{w\%-target}} \alpha_1 \sqrt{t_R} \right]^{-\frac{1}{d}}$$

Equation 5

### Response of the improved model to variations in the W/C ratio of CRFs

Figure 2 illustrates the comparison of model response in predicting UCS based on the W/C ratio for a maximum particle diameter of 2 inches, a curing time of 7 days, and three binder rates  $B_{w\%}$  (4, 6, and 8%). It is well known that the addition of water to the mix consistently results in a decrease in the strength of the backfill. Consequently, the UCS generally diminishes with an increase in the W/C ratio. From Figure 2b, it can be observed that a substantial decline is evident as the W/C ratio increases, aligning with what is expected. This improved model appears to better capture the effect of water addition on the predicted UCS through the W/C parameter.

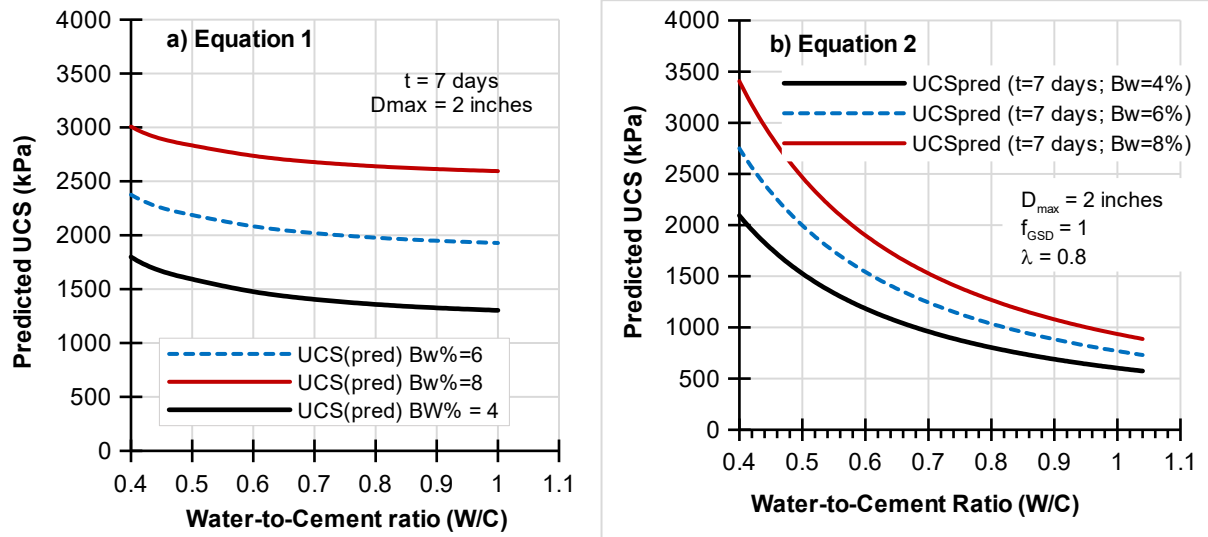


Figure 2. Comparison of the model's response in predicting UCS based on the W/C ratio for a curing time of 7 days and  $D_{\text{max}} = 2$  inches: a) original model (Equation 1), b) improved model (Equation 2).

### Response of the improved model over curing time of hardened neat cement

The curves depicted in Figure 3 illustrate the evolution of predicted UCS as a function of curing time for three water/cement ratios (0.82, 1 and 1.2). It is noteworthy that over time, the neat cement slurry hardens, leading to an increase in uniaxial compressive strength. It should be emphasized that the prediction of UCS for the W/C ratio of 0.82 could be compared to the experimental data obtained from Glencore's Raglan mine ( $\lambda = 2.12$ ,  $\alpha_{\text{GU}} = 1.4$ ). Furthermore, to achieve optimal strength, it is advisable to reduce the

water-to-cement ratio and allow sufficient curing time for the neat cement slurry. These curves showcase the capability of the improved semi-empirical model to predict UCS accurately and robustly, taking into account the influencing parameters.

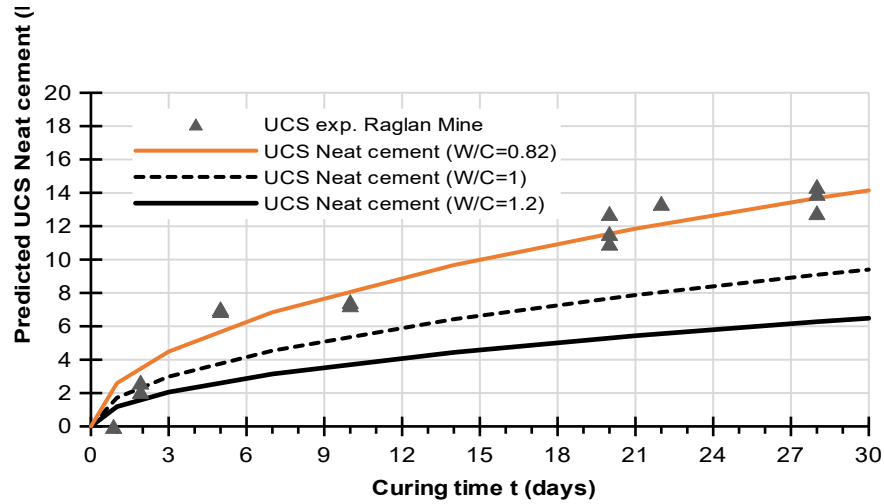


Figure 3. Predicted UCS of hardened neat cement as a function of curing time.

## Methodology

### Waste rocks

The waste rock received from the Canadian Malartic mine (CMM) exhibits a diameter range of 0–50 mm. To create mixes for cemented rock fill (CRF), the material underwent homogenization using a mechanical shovel and was stored in 20 L plastic pails. To gain deeper understanding of CRF characteristics, a sample was collected to characterize the waste rocks. Analysis revealed that the average specific gravity ( $G_s$ ) of the waste rock was 2.8. Figure 3 illustrates the particle size distribution of the waste rocks. It is noteworthy that approximately 38.8% of the particles are fine particles (diameter  $D < 10$  mm), which is crucial for achieving the desired optimal strength of the CRF (eg, Vennes, 2014).

### Binder types

For the preparation of cemented rock fill specimens, two binder types were selected: general use Portland cement (GU) and a blend of 20% of GU and 80% of ground granulated blast furnace slag (GGBFS or Slag). These two binder types are widely utilized in the mining industry due to their demonstrated effectiveness (Hassani & Archibald, 1998; Farsangi, 1996). For the preparation of neat cement slurry specimens, two binder types were employed: GU alone and GU/Slag, consisting of 55% GU and 45% Slag. These blending percentages were chosen to expedite the cement hydration process, given the limited curing time of only three days.

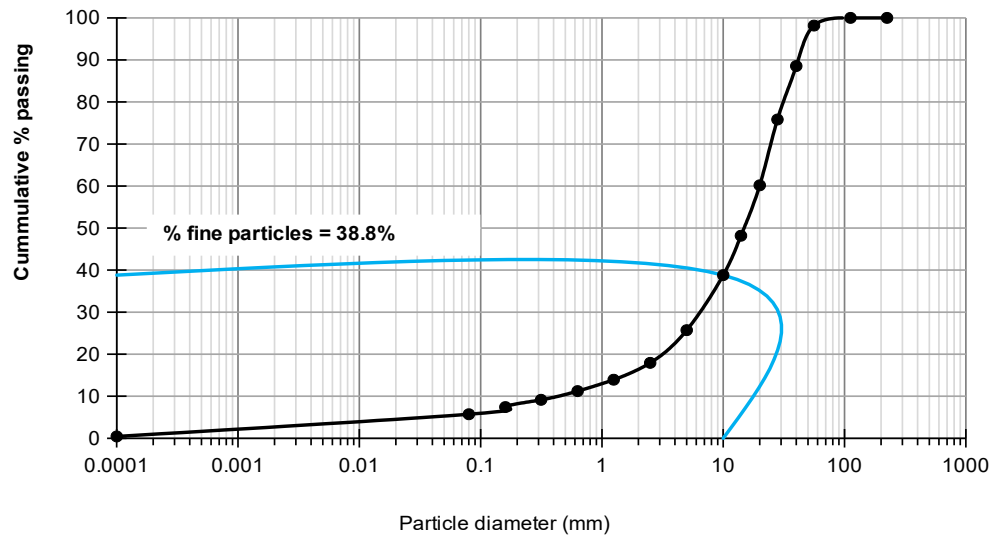


Figure 4. Particle size distribution of the waste rocks from Canadian Malartic Mine (Rafraf et al., 2023).

### Mixing water

The mixing water employed for crafting the cemented rock fill specimens originates from the municipal water supply of Rouyn-Noranda, Canada. This decision is supported by the observation that utilizing recycled mine process water has the capacity to reduce the strength of the CRF by approximately 50% in comparison to CRF produced using tap water. Additionally, the consistent availability and accessibility of tap water further contribute to the suitability of this choice (Gélinas, 2021).

### CRF mixes

The investigation employed water-to-cement ratios of 1 and 1.2 as key parameters. Additionally, three binder ratio ( $B_w\%$ ) values were explored, namely 4%, 6%, and 8%. The CRF placement porosity ( $n_{WR}$ ) was set to 0.27 (or 27%), corresponding to a void ratio ( $e_{WR}$ ) 0.37, was selected. The equivalent solids mass concentration ( $C_{w\%}$ ) ranged from 94–97%. Specimens underwent curing for two distinct times: 14 and 28 days, within a humid chamber with relative humidity (RH) > 90% and a temperature of  $22 \pm 2^\circ\text{C}$ , simulating underground conditions. Table 2 details the various recipes used in the experimentation.

Table 2. Formulation of CRF mix recipes.

Binder	Curing time (days)	Water-to-cement (W/C)	Binder ratio $B_w$ (%)	Number of specimens
GU alone / 20%GU- 80%Slag	14, 28	1	4	12
	14, 28	1	6	12
	14, 28	1	8	12
	14, 28	1.2	4	12
	14, 28	1.2	6	12
	14, 28	1.2	8	12

### Neat cement slurry mixes

The investigation involved the variation of the water-to-cement (W/C) ratio (0.8, 1.0, and 1.2) across six distinct neat cement slurry formulations. The total porosity values ( $n$ ) for placement were varied based on the W/C ratio and the relative density of the neat cement slurry ( $G_{s\text{-slurry}}$ ). Two types of binder, GU alone and 55% GU/45% Slag, were chosen. The neat cement slurry was then poured into ~ fifty small plastic molds with a diameter of 1.2 (30 mm) and 2.4 inches in height (~ 60 mm). These molds were placed in a humid chamber with a relative humidity (RH) exceeding 90% and a temperature of  $22 \pm 2^\circ\text{C}$ , mimicking underground conditions. The curing process extended over three days.

### UCS Testing

After each curing time, both CRF and neat cement molds were removed from the humid chamber and capped. Subsequently, employing a rigid mechanical press with a 100 kN loading capacity and maintaining a constant displacement velocity of 1 mm/min, the specimens underwent unconfined/uniaxial compression testing following ASTM C39/C39 M standards. The data acquisition system records axial strain and normal stress until failure, facilitating the generation of a stress-strain curve. The peak value on this curve denotes the UCS.

### Quality control methodology

To determine the ultimate water content of the CRF, the fragments from each specimen were collected, weighed, and subjected to drying after the breaking of the CRF cylinders. As a quality indicator for the CRF cast in a mold, the air void percentage ( $A_v\% = \text{volume of air}/\text{total volume}$ ) and the initial and ultimate wet densities of the test specimens were computed. Furthermore, the total/bulk and dry densities were assessed (post-casting the CRF and post-breaking), allowing for comparison with the UCS values obtained.

## Results and discussion

### Model calibration for CRF

Deriving a value of  $\alpha_{ij}$  for each binder type becomes imperative to optimize the effectiveness of the improved semi-empirical prediction model (Equation 2) for predicting the strength of cemented rock fill. The primary emphasis is on fitting two distinct values, one tailored for the GU-type binder and the other for the GU-Slag binder. Table 3 presents the results obtained from the Python code employed for model calibration, taking into consideration the breaking outcomes of the CRF specimens.

Table 3. Different fitting values of  $\alpha_{ij}$  for the two types of binder.

Binder type	GU	20% GU / 80% Slag
$\alpha_i$ values ( $j = 1 = \text{CRF}$ )	2.27	1.89

Figures 5 and 6 illustrate histograms displaying both the experimental and predicted UCS values. Emphasizing the capability of the improved semi-empirical model to accurately forecast strength for both types of binder, it integrates key parameters associated with the formulation of cemented rock fill recipes. In practical terms, the outcomes are influenced by variables including the water-to-cement ratio ( $W/C$ ), binder ratio ( $B_w\%$ ) and curing time ( $t$ ). The histogram's juxtaposition of predicted and experimental values underscores a substantial agreement between the two sets of data.



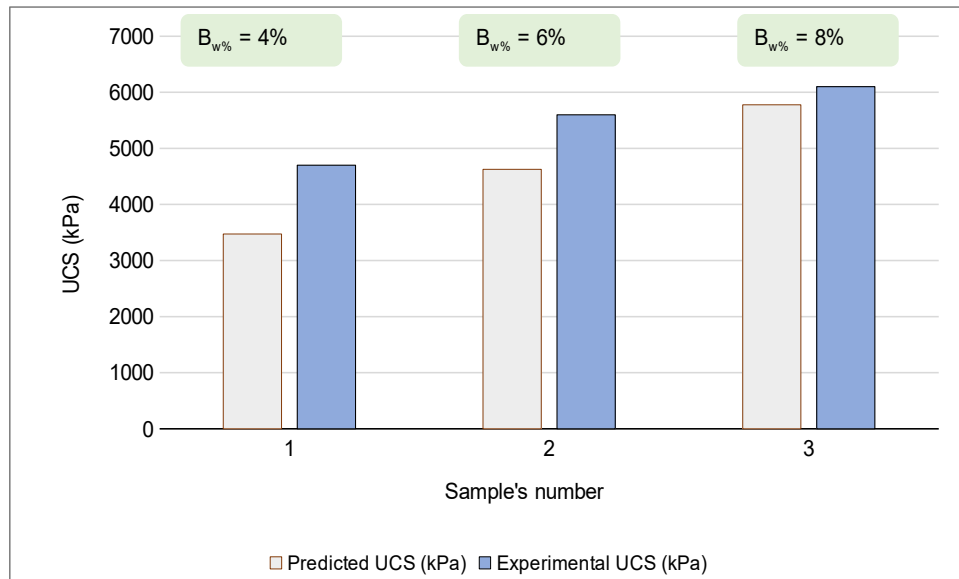


Figure 5. Comparison between predicted and experimental UCS of CRF prepared with GU cement, under conditions of W/C of 1 and curing time (t) of 28 days.

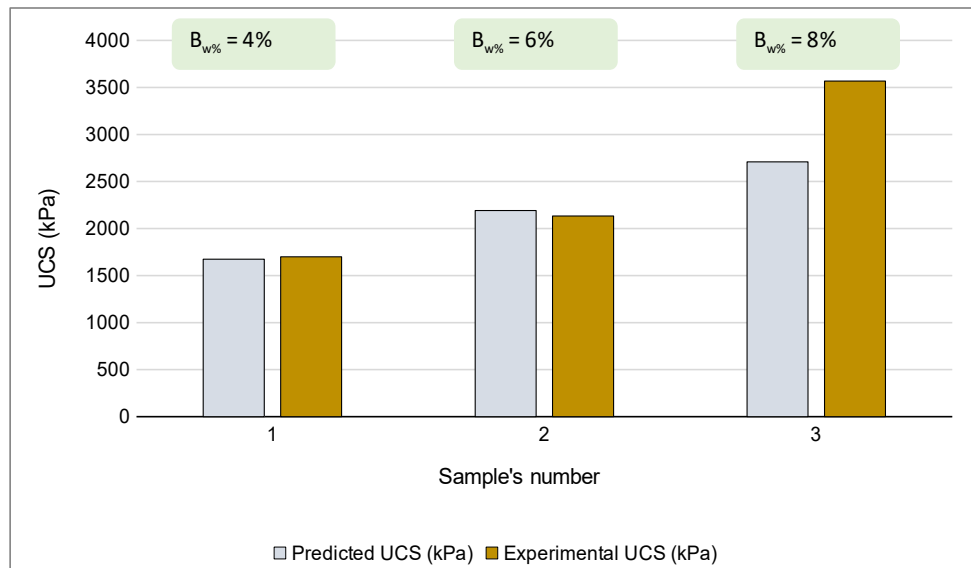


Figure 6. Comparison between predicted and experimental UCS of CRF prepared with GU-Slag binder, under conditions of W/C of 1 and curing time (t) of 14 days.

## Performance metrics of the UCS prediction of the CRF

### Linear regression

To enhance the assessment the improved semi-empirical model's predictive capability for UCS, the linear regression correlation coefficient is computed. The correlation coefficient (R) is derived from the following equation:

$$R = \frac{\sum_{j=1}^N (y_j - \bar{y}_j)(\hat{y}_j - \bar{\hat{y}}_j)}{\sqrt{\sum_{j=1}^N (y_j - \bar{y}_j)^2} \sqrt{\sum_{j=1}^N (\hat{y}_j - \bar{\hat{y}}_j)^2}}$$

Equation 6

where  $y_j$  represents the experimental values,  $\hat{y}_j$  stands for the predicted values,  $\bar{y}_j$  is the average of the experimental values, and  $\bar{\hat{y}}_j$  is the average of the predicted values.

A higher correlation between the predicted and experimental UCS is indicated when the correlation coefficient (R) approaches 1. The linear regressions illustrating the relationship between the experimental and predicted UCS values for the two types of CRF mixes are presented in Figure 7.

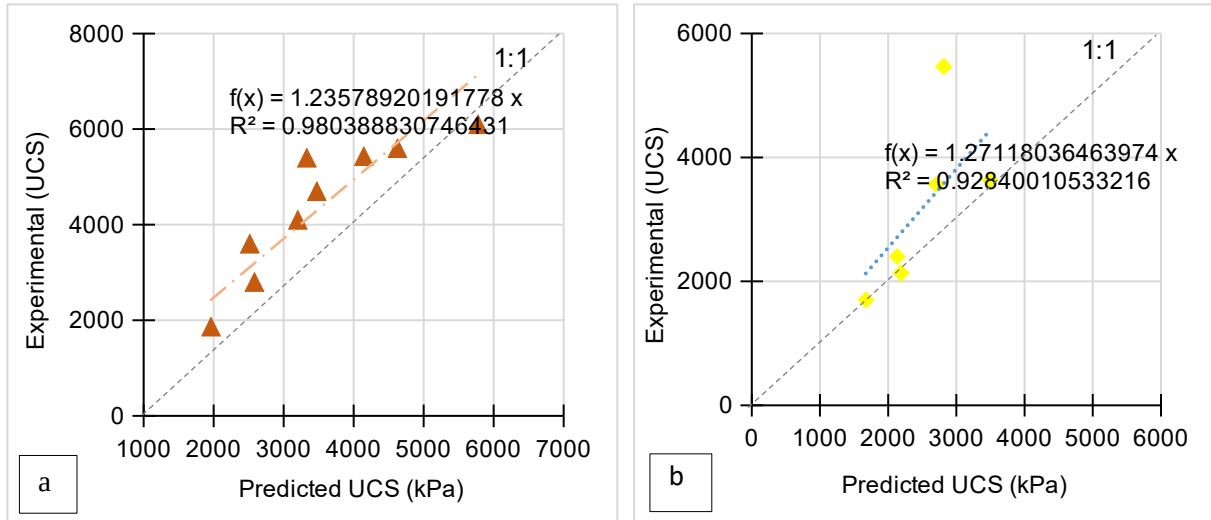


Figure 7. Linear regression curves a) for the GU cement, and b) for 20GU/80Slag binder.

Remarkably, in the case of CRF prepared with de GU cement, the data points illustrating the relationship between the two sets of values are closely aligned around the linear regression line. Additionally, the coefficient of determination ( $R^2$ ) is calculated to be 0.9804, corresponding to a correlation coefficient (R) of 0.99. For the GU-Slag type of binder, although two points are somewhat scattered, most of the points closely adhere to the linear regression line, yielding a correlation coefficient (R) of 0.96. These findings underscore the efficiency and robustness of the model in predicting the UCS of cemented rockfills.

A small application was built to assess model calibration by determining the optimal value of  $\alpha_{ij}$ , a parameter closely linked to the binder ratio.

#### *Model Calibration for Neat Cement Slurry Strength*

To develop a reliable tool for predicting the uniaxial compressive strength of neat cement slurries (water + cement), it is pertinent to fine-tune the constant, considering distinct outcomes for the two tested binder types. Table 4 presents the specific values associated with each type of binder, while Table 5 compares the experimental and predicted UCS values for different neat cement formulations.

Table 4. Different fitting values of  $\alpha_{ij}$  for the two types of binder.

Binder type	GU	55% GU / 45% Slag
$\alpha_i$ values (j = 0 = neat cement)	3.3	1.2

Table 5. Comparison of experimental and predicted UCS values across various neat cement formulations.

Binder Type	W/C	t (days)	UCS <sub>pred</sub> (kPa)	UCS <sub>exp</sub> (kPa)	(UCS <sub>pred</sub> – UCS <sub>exp</sub> ) (kPa)
GU-Slag	0.8	3	3782.4	3199.4	583.0
	1	3	2445.5	2513.4	-67.9
	1.2	3	1733.2	2231.7	-498.5
GU	0.8	3	10925.1	12717.8	-1792.7
	1	3	7011.5	8388.4	-1376.9
	1.2	3	4942.2	5973.5	-1031.3

#### **Performance Metrics of the UCS Prediction of the Neat Cement Slurry**

The effectiveness of the improved semi-empirical model in predicting the uniaxial compressive strength of the neat cement is assessed through the examination of linear regression curves.

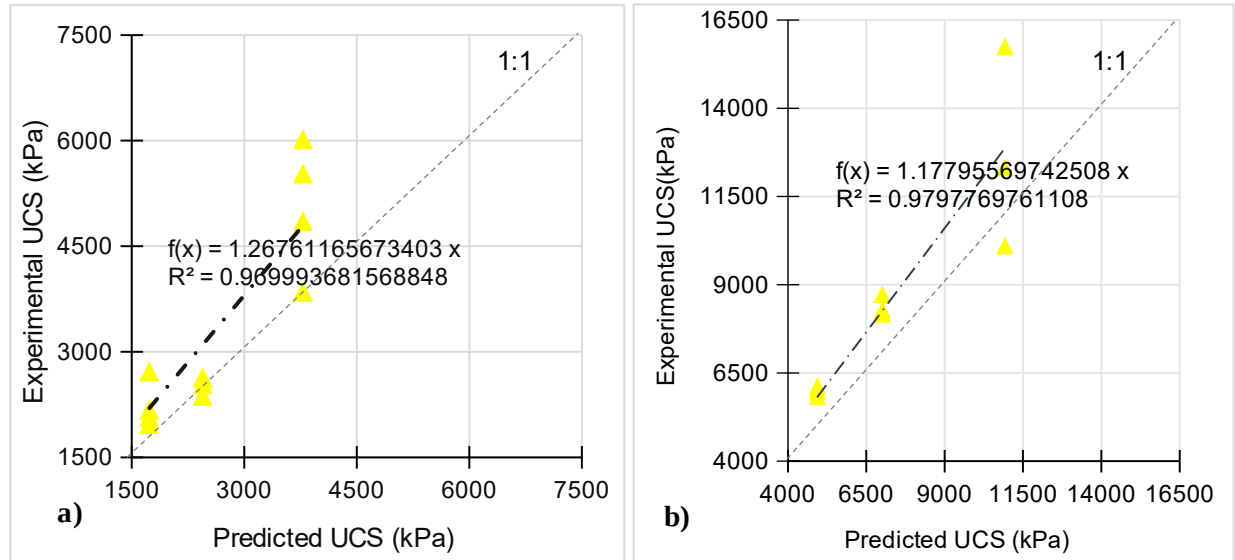


Figure 8. Linear regression curves, a) for the GU/Slag binder, and b) for GU binder.

In the case of both binder types, the linear regressions illustrated in Figure 8 demonstrate a robust correlation between the experimental and predicted values. Specifically, the data points align closely with the linear regression line, indicating a strong relationship. Notably, the coefficient of determination ( $R^2$ ) stands at 0.97, and the correlation coefficient ( $R$ ) is 0.98, approaching unity. This observation suggests a high degree of resilience in the model.

### Quality Control Methodology

#### *Relationship Between Air Voids and the UCS*

A notable correlation was observed between the percentage of air voids and the uniaxial compressive strength of cemented rock fill. The presence of air in cemented rock fill was found to directly influence its strength, introducing potential weak points in its structural composition. It is advisable to monitor the compaction process of fabricated cemented rockfills. Figure 9 shows this correlation for selected samples.

#### *Final Gravimetric Water Content*

The highest gravimetric water content at final stage ( $W_{\text{final}\%}$ ) is inversely correlated with the lowest uniaxial compressive strength. This correlation underscores that the presence of water, both in backfill mixes in general and specifically in cemented rockfill, inevitably leads to a reduction in strength. Such a reduction can significantly impact the stability and longevity of structures, as depicted in Figure 10. Notably, at a water-to-cement ratio of 1.2, cemented rockfill mixes exhibit a larger final water content, given their inherent higher water proportion. This outcome emphasizes the direct influence of water-to-cement ratio on the final classification of cemented rock fill. To ensure the attainment of the required strength, vigilant monitoring of the final gravimetric water content in cemented rock fill is essential, as illustrated in Figure 11.

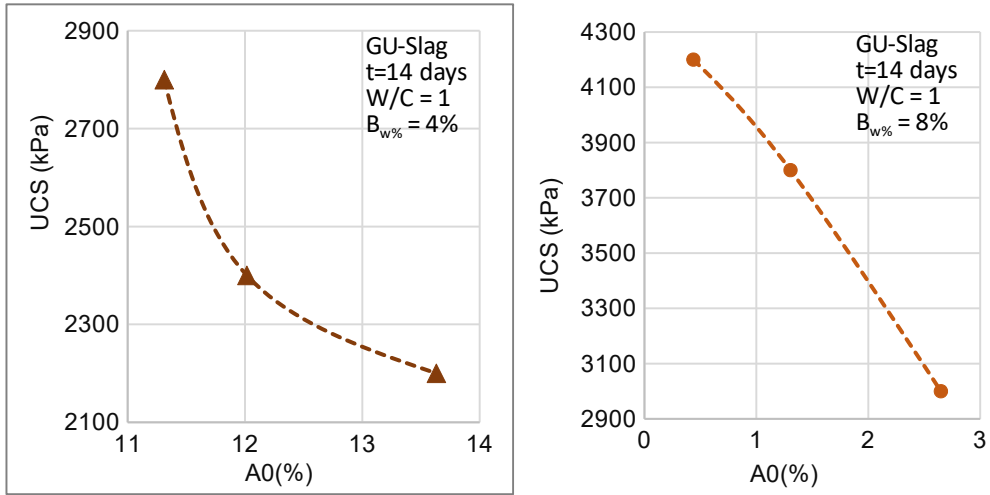


Figure 9. Variation in UCS as a function of  $A_0$  (%) for CRF prepared with GU-Slag binder.

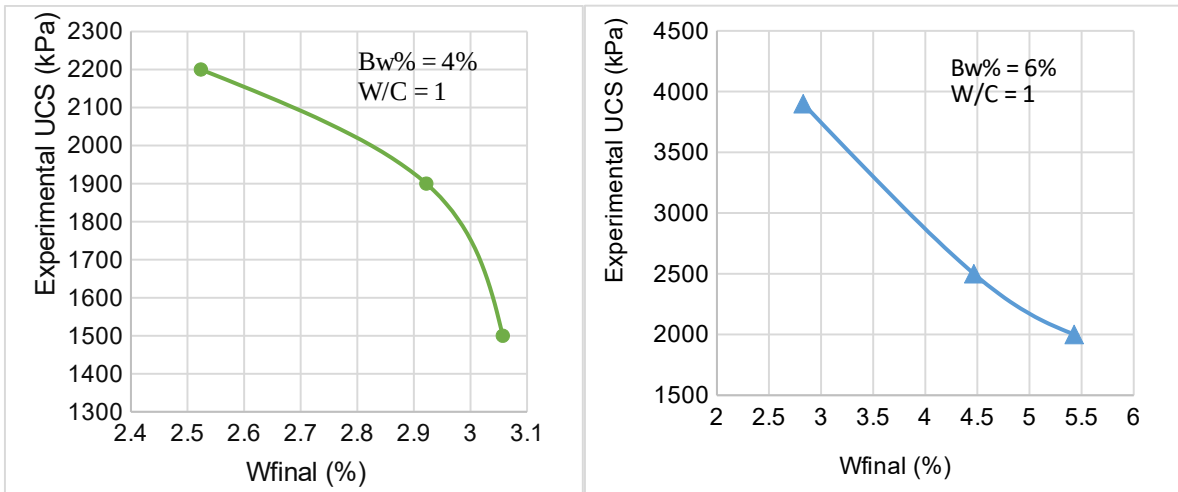


Figure 10. Variation in UCS as a function of  $W_{final}$  (%) for CRF prepared with GU cement and at curing time of 14 days.

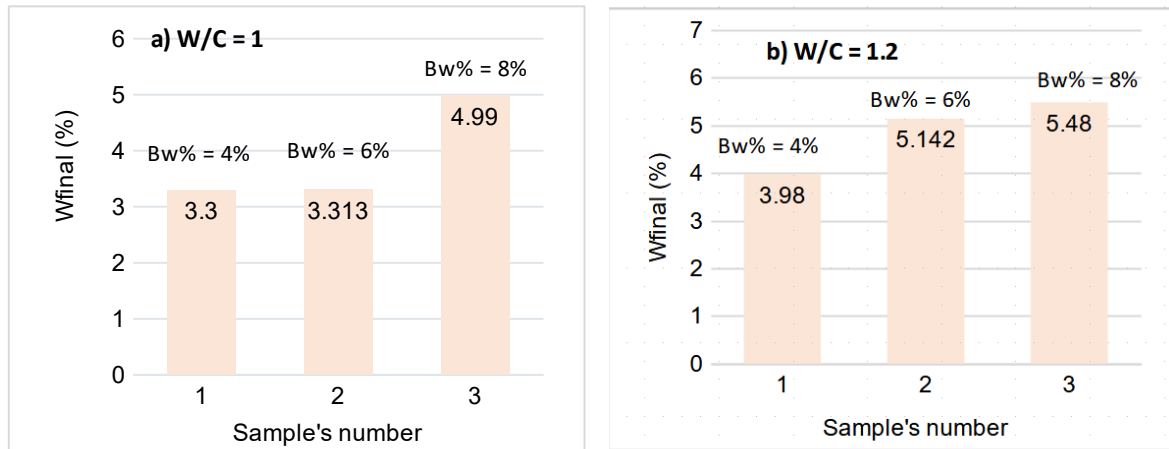


Figure 11. Variation in final gravimetric water content percent of CRF prepared with GU-Slag binder for a curing time of 14 days.

## Conclusion

This research aims to experimentally validate an improved semi-empirical model for predicting the UCS of both CRF and hardened neat cement. Key conclusions drawn from this study include:

- The improved prediction model incorporates various mixes and geotechnical parameters (such as curing time, binder ratio, particle size distribution, water-to-cement ratio, binder type, and porosity) to accurately predict the strengths of cemented rock fill, ensuring a comprehensive approach.
- Strong correlations observed between the experimental and predicted UCS values. Specifically, a correlation coefficient ( $R$ ) of 0.99 was noted for CRF made with GU cement, and  $R = 0.96$  for CRF made with GU-Slag binder, indicating the robustness of the model.
- The study revealed significant correlation between the experimental and predicted UCS values for hardened neat cement, with correlation coefficients of 0.97 for GU neat cement and 0.98 for GU-Slag neat binder. These results emphasize the reliability of the improved semi-empirical prediction model for neat cement slurry.
- Despite an W/C ratio of 1.2 falling within the industry-recommended range for designing cemented rockfill, the study suggests that considering a variation range of 0.7–1 may be beneficial to maximize the formulations for cemented rock fill.
- The lithology of the waste rock used in the design of cemented rockfills must be carefully considered. Additionally, incorporating a safety margin is advisable to ensure the long-term stability of the backfill mass.

## References

- ASTM C39/C39M–12 (2012). Standard test method for compressive strength of cylindrical concrete specimens. ASTM International.
- Amaratunga, L. M., Yaschyshyn, D. N. (1997) Development of a High Modulus Paste Fill Using Fine Gold Mill Tailings. *Geotechnical & Geological Engineering* 15:205-19.

- Annor, A.B (1999). A study of the characteristics and behaviour of composite backfill material, Ph.D. Thesis, McGill University, 396 p.
- Arioglu E. (1984). Design aspects of cemented aggregate fill mixes for tungsten stoping operations. *Mining science and technology*: 209-214.
- Association minière de Québec - AMQ (2018). Retombées économiques de l'industrie minière au Canada. [Association\\_miniere\\_du\\_Qubec\\_i\(prnewswire.com\)](http://Association_miniere_du_Qubec_i(prnewswire.com))
- Aubertin, M., Bussière, B. (2002) La gestion des rejets miniers dans un contexte de développement durable et de protection de l'environnement. Congrès annuel de la Société canadienne de génie civil
- Aubertin, M., Bussière, B., Bernier, L. (2002) Environnement et Gestion Des Rejets Miniers. Presses Internationales Polytechniques, CD-ROM, Montréal
- Belem T. (2020). Semi-empirical models for predicting the unconfined compressive strength of virtual un-cemented rockfill (RF) and cemented rockfill (CRF). Research Institute on Mines and Environment (RIME) Internal Report 19 p.
- Belem T. (2023). Improved semi-empirical model for predicting the unconfined compressive strength of cemented rockfill (CRF) and hardened neat cement strength. Research Institute on Mines and Environment (RIME) Internal Report, 15 p.
- Bussière, B. (2007). Colloquium 2004: Hydrogeotechnical properties of hard rock tailings from metal mines and emerging geoenvironmental disposal approaches. *Canadian Geotechnical Journal*, v. 44, no. 9, p. 1019-1052.
- Farsangi, P.N. (1996). Improving Cemented Rockfill Design in Open Stopping. Ph.D. Thesis, McGill University, Montreal, 340 p.
- Farsangi P.N., Hayward A.G., Hassani F.P. (1996). Consolidated rockfill optimization at Kidd Creek Mines. *CIM Bulletin*, 89:129–134.
- Fuller, W. B., & Thompson, S. E. (1907). The laws of proportioning concrete. *Transactions of the American Society of Civil Engineers*. 57(2).
- Gélinas, LP. (2021). Current knowledges on arctic cemented rockfill (CRF) cured in permafrost conditions. Internal AEM document #6128-000-100-TCR-001. Technical report.
- Gonano, LP, Kirkby, RW, & Dight, PM (1978). Triaxial testing of cemented rockfill. *Technical Report 72*, CSIRO, Australia.
- Hane, I., Belem, T., Bemzazoua, M. (2018). Cemented Rockfill (CRF) Plant Laboratory Test. Unité de recherche et de service en technologie minérale. 20 p.
- Hedley, DG F. (1995). Final report on the stiff backfill project for M.R.D., Mining Research Directorate, Canadian Rockburst Research Program, Sudbury, Ontario.
- Lamos, A., Clark, I. (1989). The influence of material composition and sample geometry on the strength of cemented backfill. Hassani FP, Scoble MJ, Yu TR, eds. *Innovations in Mining Backfill Technology*. Brookfield (USA): AA Balkema Publishers, 89-94.
- Mitchell. R. Wong. B (1982). Behaviour of cemented tailings sands. *Canadian Geotechnical Journal*. 19 (3). 289-295.
- Rafraf, G., Belem, T., Mrad, T., Gélinas, LP., Krichen, A. (2023). Experimental validation of a prediction model of the compressive strength of cemented rock fills. in GW Wilson, NA Beier, DC Sego, AB Fourie & D Reid (eds), *Paste 2023: Proceedings of the 25th International Conference on Paste, Thickened and Filtered Tailings*, University of Alberta, Edmonton, and Australian Centre for Geomechanics, Perth, pp. 841-852, [https://doi.org/10.36487/ACG\\_repo/2355\\_67](https://doi.org/10.36487/ACG_repo/2355_67).
- Talbot, A. N., & Richard, F., 1923. The Strength of Concrete: Its Relationship to the Cement, Aggregates and Water. *Expr. Stat. Bull*, 137.
- Vennes, I (2014), Determination of Cemented Rockfill Strength with Large Scale UCS Tests under In-Situ Conditions. Thesis, McGill University, 100 p.

Stone. DMR 2007. Factors that Affect Cemented Rockfill Quality in Nevada Mines. CIM Bulletin. vol. 100. No. 1103. pp. 1-6.

Yu. T (1989). Some factors relating to the stability of consolidated rockfill at Kidd Creek. Innovations in Mining Backfill Technology. 279-286.